ULTIMATE LOAD-DEFLECTION CHARACTERISTICS AND FAILURE MODES OF CEILING DIAPHRAGMS FOR FARM BUILDINGS

K. G. Gebremedhin and *W. W. Irish*

Assistant Professor and Professor
Department of Agricultural Engineering
Cornell University, Ithaca, NY 14853

(Received August 1985)

ABSTRACT

Load-deflection characteristics and failure modes of metal-clad, timber-framed, screw-fastened ceiling diaphragms are presented. Diaphragms, 2.44 m × 6.10 m (8 ft × 20 ft) and 2.44 m × 4.88 m (8 ft × 16 ft), were built and tested as deep beams. Loads were applied to simulate wind loads on ceilings of farm buildings. Variables included panel profile, rib orientation, size of supporting grid, diaphragm size, spacing of end-fasteners, and effect of an opening at midspan.

Keywords: Ceiling diaphragm, deep beam, in-plane loading, diaphragm strength, load-deflection, failure mode, metal sheathing.

INTRODUCTION

In-plane shear forces develop in ceilings of metal-clad buildings due to wind. Light-gage metal ceiling systems, if properly built, can transfer in-plane shear forces to the end walls with little deformation in the ceiling. The entire ceiling acts as a large, deep beam to transmit lateral wind forces to the ends of the building by diaphragm action.

Previous work (Luttrell 1967; Hausman and Esmay 1977; White 1978; Hoagland and Bundy 1983; Johnston and Curtis 1984) related to diaphragm load-deflection characteristics involved testing roof or ceiling diaphragm components loaded as cantilever systems. In agricultural buildings, where the roof or ceiling length-to-width ratio is large, deep beam action (bending) becomes an important design parameter of wall column design (Gebremedhin and Woeste 1985). A midspan deflection of up to 51 mm (2 in.) at a 71 kN (15,962 lb) load was reported by Turnbull et al. (1982) for ceiling diaphragms of farm buildings. Thus, the lateral midspan deflection of a roof or ceiling diaphragm must be checked to ensure that the deflection is small.

Diaphragm response to load is dependent on several variables including panel profile, type, and spacing of fasteners, diaphragm size, cover width, material strength, size of supporting grid, the loading regime, etc. Because of the large number of variables, theoretical determination of diaphragm behavior is extremely complex. Diaphragm behavior usually is determined on the basis of test panels representing typical roofing or ceiling sections. This paper presents in-plane strength data and mode of failure of ceiling diaphragms used in farm buildings.

This study simulates wind loads on ceiling diaphragms of farm buildings. The objectives were:

1. To determine the load-deflection characteristics and failure modes of metal-clad, timber-framed, screw-fastened ceiling diaphragms tested as deep beams.

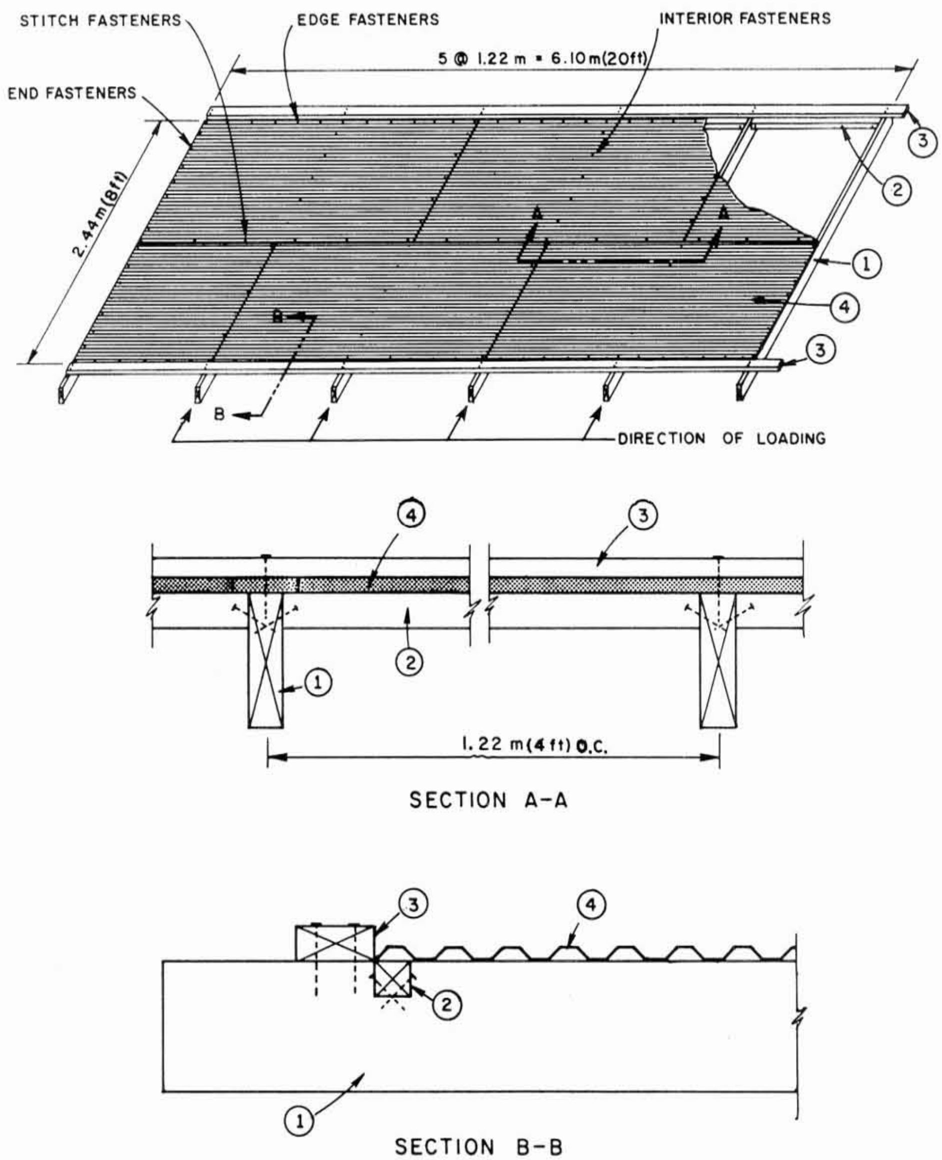

FIG. 1. Test frame and details. (1) 38 mm × 140 mm (2 × 6) members representing ceiling joists or roof trusses; (2) 38 mm × 38 mm (2 × 2) nailers; (3) 89 mm × 38 mm (4 × 2) beam edge; (4) metal sheathing.

2. To investigate effects of: (i) panel profile, (ii) rib orientation, (iii) size of diaphragm, (iv) size of supporting grid, (v) spacing of end-fasteners, and (vi) an opening at midspan, on the strength and mode of failure of ceiling diaphragms.

DIAPHRAGM CONSTRUCTION AND TESTING PROCEDURE

Framing

Framing simulated ceiling diaphragms consisting of (1) 38 mm × 140 mm (2 × 6) members simulating ceiling joists or lower chords of trusses 1.22 m (4 ft)

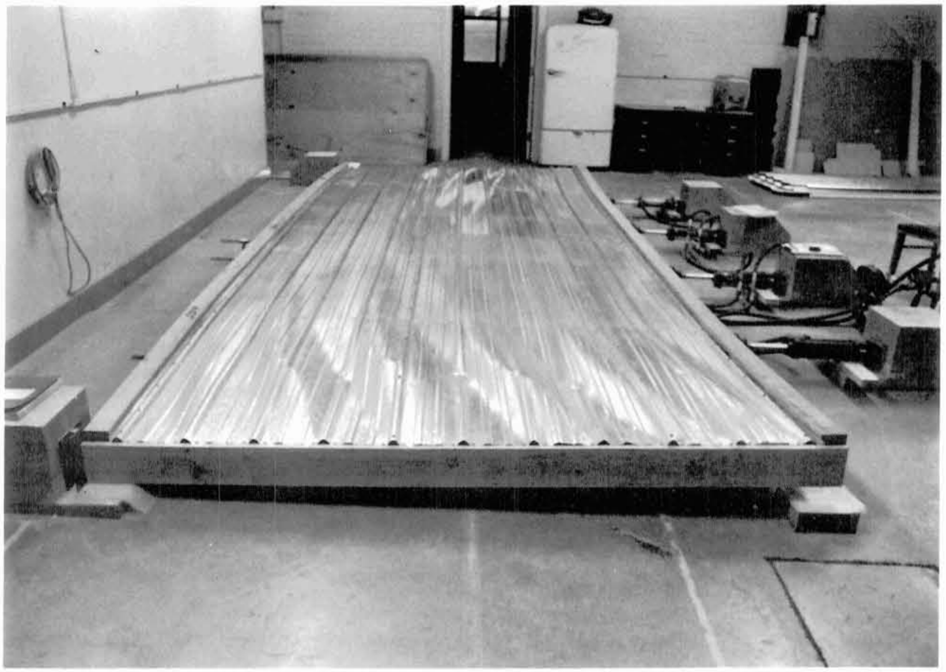

FIG. 2. Loading system and end supports. Also shown are 5 to 6 ripples starting from the ends and propagating towards the center.

o.c.; (2) 38 mm × 38 mm (2 × 2) nailers, toe-nailed between chords with 2-8d nails at each end; and (3) 89 mm × 38 mm (4 × 2) beam edge nailed flat to the chords by 2-10d nails (Fig. 1). The truss chords were placed on edge and were supported horizontally on a concrete pad at the two ends (Fig. 2). When metal panels were laid down with ribs parallel to truss chords, additional 89 mm × 38 mm (4 × 2) blocking toe-nailed by 2-8d nails between chords at one-third or one-half diaphragm width were included.

The truss chords were No. 2 and better grade Douglas-fir at ≤19% moisture content. The edge beams and blockings were construction grade Douglas-fir.

Metal cladding

One profile of aluminum and two profiles of galvanized steel were used in this study. Aluminum panels were 0.018 gage, 14 mm (9/16 in.) deep, equally spaced diamond-embossed rib profile. One profile of the galvanized steel panels was 29 gage, twin 11 mm (7/16 in.) deep ribs spaced 203 mm (8 in.) on center. The second profile of galvanized steel panels was 29 gage with 19 mm (3/4 in.) deep major ribs spaced 228 mm (9 in.) on center. Profiles, widths, and coverage of these panels is illustrated in Fig. 3. All panels and fasteners were obtained from commercial stock.

Fasteners

Panel-to-frame fasteners along the long edges of the diaphragm (edge-fasteners) were 51 mm (2 in.) long #11 wood-grip, self-drilling aluminum screws, spaced 203 mm (8 in.) on center. Panel-to-frame fasteners along the two ends of the

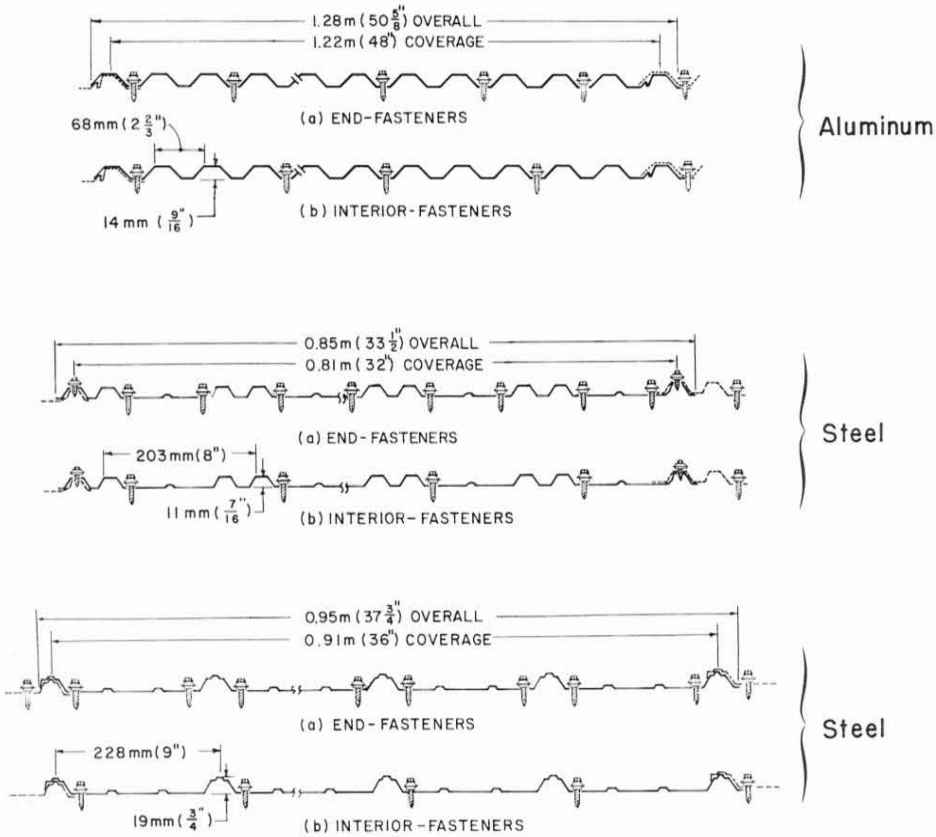

FIG. 3. Panel profiles, cover width, and spacing of fasteners.

diaphragm (end-fasteners) were 25 mm (1 in.) long #8 wood-grip, self-drilling zinc-coated carbon steel screws, spaced every second valley (Fig. 3). Panel-to-frame fasteners along the intermediate supports (interior-fasteners) were the same as those of the end-fasteners, but spaced every third valley (Fig. 3). Sidelap stitch fasteners were 16 mm (⅝ in.) long, #12 self-drilling, self-tapping cadium-plated steel screws spaced 457 mm (18 in.) on center. These connectors pass only through the two lapped sheets to transfer shear from panel to panel.

The edge-fasteners and the stitch screws were applied through the ribs, but the end-fasteners and interior-fasteners were applied at the flat surfaces (valley). All screws included a metal/neoprene composite bonded washer for weather tightness. The screws were driven with an electric screw gun with a depth-setting nose piece to prevent under- or over-driving.

Loading

Four identical hydraulic cylinders connected in parallel and located in the plane of the chords (Fig. 2) loaded the diaphragm. Line pressure was applied in increments of 67 kN/m^2 (10 psi) at 3 min intervals until failure. The hydraulic cylinders had calibration differences of less than 6%; 1 kN/m^2 = 3.2 N (1 psi = 4.9 lb) load. Dial deflection gages indicated in-plane deflections at midspan and at 1.22 m (4 ft) from each end of the diaphragm.

All modules were built and tested with the sheeting on top to simplify fabrication and to better observe the effects of loading.

The loading procedure was:

1. Apply an initial 67 kN/m^2 (10 psi) line pressure to force the diaphragm to "constant" position, and then record initial deflections on the deflection dial gages.
2. Apply 345 kN/m^2 (50 psi) line pressure, and record deflections.
3. Increase line pressure by 67 kN/m^2 (10 psi) increments every 3 min, recording deflections and any structural behavior at each increment.
4. Stop loading when deflection increased with no detectable increase in pressure or when permanent damage occurred. The above procedure was followed during testing. Twelve 2.44 m × 6.10 m (8 ft × 20 ft) and four 2.44 m × 4.88 m (8 ft × 16 ft) diaphragms were tested. These sizes include aspect ratios (length-to-width ratio) of 2.5 and 2.0, which are typical in farm buildings.

RESULTS AND DISCUSSION

Load applied parallel to ribs

The relationships between load-to-in-plane deflection for three tests, when loads were applied parallel to ribs or when panels were fastened parallel to the supporting chords, are shown in Fig. 4. The total in-plane load (P_u) and midspan deflection (Δ) at failure were: aluminum, P_u = 25.9 kN (5,823 lb), Δ = 26 mm (1.02 in.); steel 11 mm (7/16 in.) deep ribs, P_u = 28.7 kN (6,452 lb), Δ = 27.8 mm (1.09 in.); and steel 19 mm (3/4 in.) deep ribs, P_u = 30 kN (6,744 lb), Δ = 26 mm (1.02 in.). At failure, the diaphragm fabricated with aluminum was weaker by 11 to 16% than that of steel. Strength is defined as the maximum in-plane load carried by the diaphragm before failure occurred.

The mode of failure was the same in all three tests, and can be characterized according to the following stages:

1. Formation of ripples at end panels started at 50% of P_u for aluminum and at 75% for steel.
2. Tilting of stitch screws at the first lap joints.
3. Accordion-like warping across the panel ends that gradually propagated to, but never reached, the middle 1.22 m (4 ft) span. Angle of warp was less than diagonal. Warping of the metal was pronounced at the first and last 1.22 m (4 ft) spans, and relatively moderate at the second and fourth spans, leaving the center one fifth span unaffected. Up to six ripples appeared before failure.
4. Failure was by mild tearing and popping out of stitch screws, at sidelaps close to the ends of the diaphragm, and screw withdrawal at end-fasteners (Fig. 5). Tearing around stitch screws and end-fasteners was more pronounced in aluminum than in steel.

Effect of size of supporting grid on strength and mode of failure

Two additional tests were performed on aluminum with different support grid size. These tests include 89 mm × 38 mm (4 × 2) blocking, spaced to make the support grid 0.81 m × 1.22 m (2 ft 8 in. × 4 ft) instead of 1.22 m × 1.22 m (4

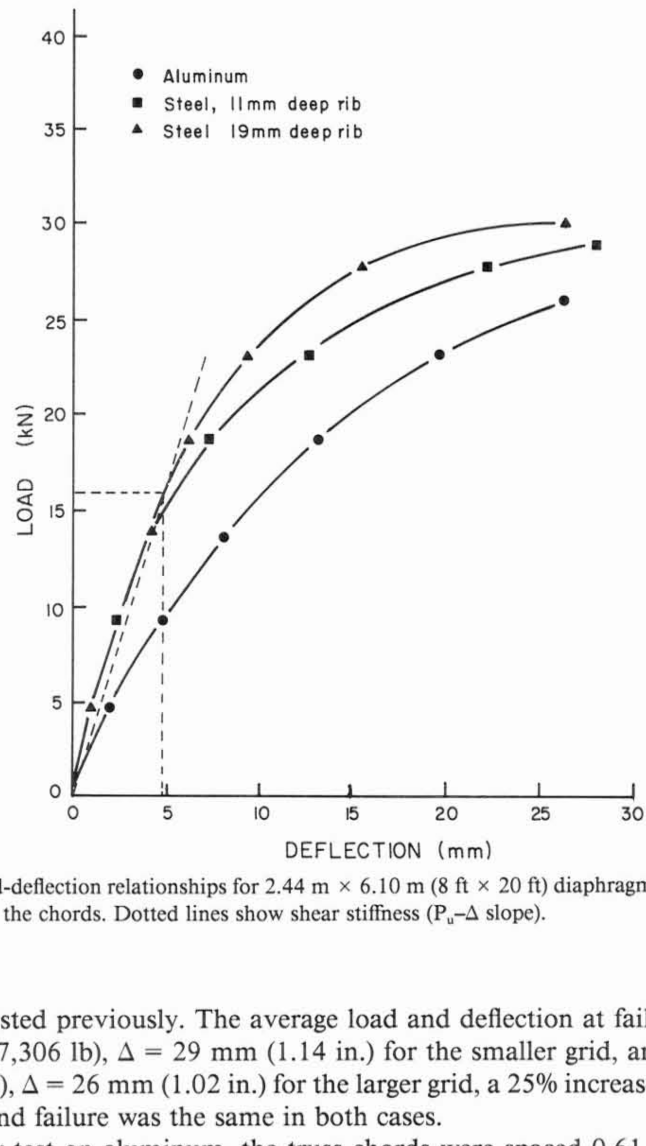

FIG. 4. Load-deflection relationships for 2.44 m × 6.10 m (8 ft × 20 ft) diaphragms when the ribs were parallel to the chords. Dotted lines show shear stiffness (P_u–Δ slope).

ft × 4 ft), tested previously. The average load and deflection at failure were: P_u = 32.5 kN (7,306 lb), Δ = 29 mm (1.14 in.) for the smaller grid, and P_u = 25.9 kN (5,823 lb), Δ = 26 mm (1.02 in.) for the larger grid, a 25% increase in strength. The mode and failure was the same in both cases.

In another test on aluminum, the truss chords were spaced 0.61 m (2 ft) o.c. instead of 1.22 m (4 ft) to make the supporting grid 0.81 m × 0.61 m (2 ft 8 in. × 2 ft). The load and midspan deflection at failure between that and the 0.81 m × 1.22 m (2 ft 8 in. × 4 ft) grid were unchanged. P_u = 33 kN (7,419 lb), and Δ = 28 mm (1.10 in.). The P_u–Δ relationships of the three supporting grid sizes are shown in Fig. 6. The loads and midspan deflections of all the tests are given in Table 1.

Load applied perpendicular to ribs

Load-deflection relationships of three 2.44 m × 6.10 m (8 ft × 20 ft) diaphragms loaded perpendicular to ribs are shown in Fig. 7. The load and midspan deflection at failure were: aluminum, P_u = 30.6 kN (6,880 lb), Δ = 34 mm (1.34 in.); steel 11 mm ($^7/_{16}$ in.) deep rib, P_u = 39.8 kN (8,948 lb), Δ = 36 mm (1.42 in.); and

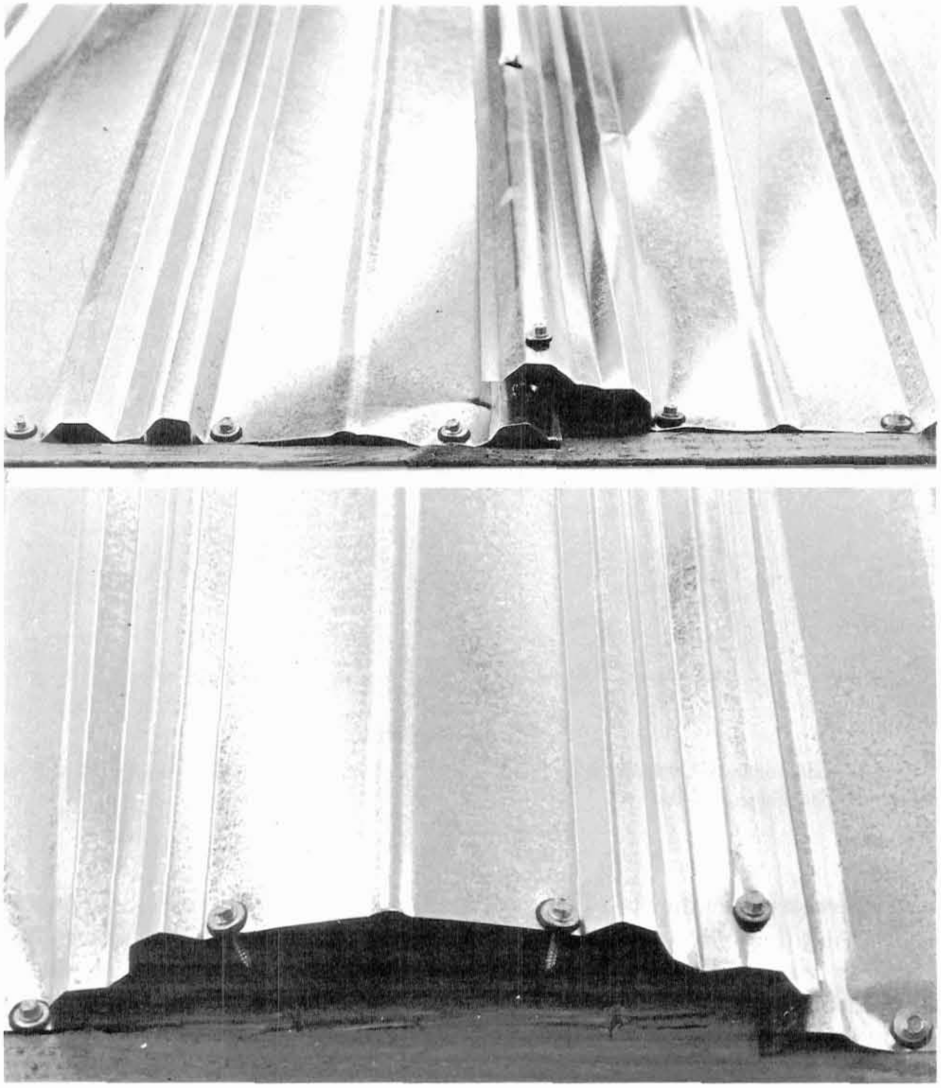

FIG. 5. (a) Failure by tearing and popping out of stitch screws, and (b) withdrawal at end-fasteners.

steel 19 mm (¾ in.) deep rib, $P_u = 39.3$ kN (8,835 lb), $\Delta = 34$ mm (1.34 in.). Both steel diaphragms failed at approximately the same load and deflection, and were stronger than their aluminum counterpart by 29%.

Aluminum panels fastened with ribs perpendicular to the supporting chords were 18% stronger than when ribs were parallel. In the steel diaphragms, the increase in strength was 24% for the 11 mm ($^7/_{16}$ in.) deep rib, and 39% for the other. The increase may be due to rib resistance to bending when the load was applied perpendicular to the ribs. When the load was applied parallel, the ribs contributed little bending resistance because of bellows action.

Further comparison of Figs. 4 and 7 shows that rib orientation affects not only strength but even more significantly shear stiffness (P_u–Δ slope). When steel panels

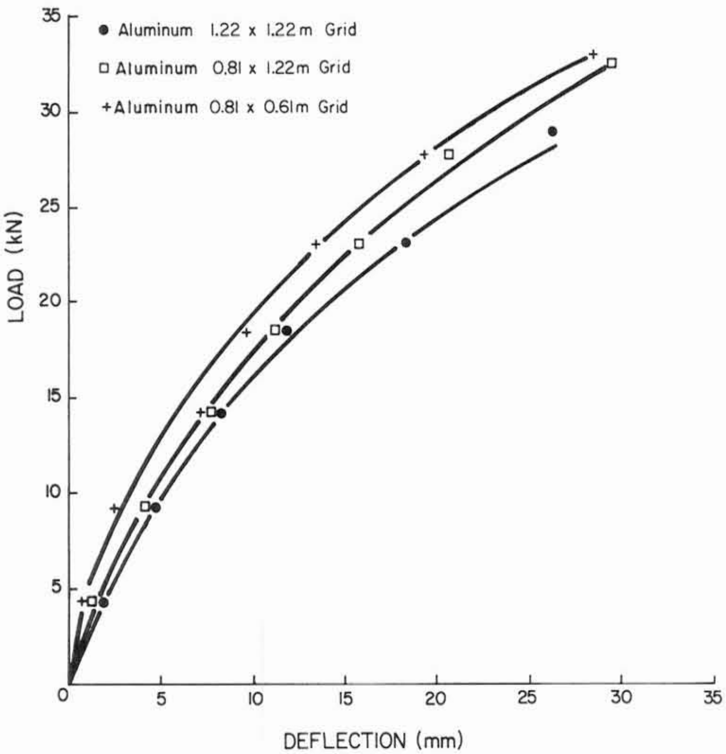

FIG. 6. Load-deflection relationships for 2.44 m × 6.10 m (8 ft × 20 ft) diaphragms of three different supporting grid sizes.

were fastened perpendicular to the supporting chords (Fig. 7), the P_u–Δ slope was nearly twice that of when parallel (Fig. 4). The shear stiffness may be determined from the nearly linear region of the P_u–Δ curve (dotted lines in Figs. 4 and 7). Shear stiffness is more relevant for the design of wall members subjected to a racking load. Luttrell's (1967) formula can be used to convert panel stiffness data from a given length to other lengths.

Based on three tests, the mode of failure of panels supported perpendicular to ribs can be characterized according to the following stages:

1. Pile up or roll up of material ahead of fasteners started at 42% of P_u for aluminum and at 51% for steel diaphragms.
2. Accordion-like warping (5 to 6 ripples) appeared across the diaphragm at 75% of P_u. The ripples started at both ends and gradually propagated but never reached the middle 1.22 m (4 ft) span. Further loading initiated warping of the 89 mm × 38 mm (4 × 2) edge beams causing downward bowing at the tension edge and upward bowing at the compression edge.
3. Tilting of stitch screws at sidelaps close to the ends of the diaphragm and tearing of panels around the stitching screws.
4. Failure was by local panel kinking along several ripples, and popping out of screws along the two ends. Kinks were inelastic and occurred within 305 mm to 457 mm (12 to 18 in.) from the ends.

TABLE 1. *Comparison of load (P_u) and midspan deflection (Δ) of ceiling diaphragms at failure.*

Diaphragm size (m)	Loading direction	Support trusses o.c. (m)	Grid size blocking o.c. (m)	Aluminum		Steel 11-mm-deep rib		Steel 19-mm-deep rib	
				P_u (kN)	Δ (mm)	P_u (kN)	Δ (mm)	P_u (kN)	Δ (mm)
Effect of grid size									
2.44 × 6.10	∥[1] to ribs	0.61	0.81	33	28				
2.44 × 6.10 (2)[3]	∥ to ribs	1.22	0.81	32.5	29				
2.44 × 6.10	∥ to ribs	1.22	1.22	25.9	26				
Effect of rib orientation									
2.44 × 6.10	∥ to ribs	1.22	1.22	25.9	26	28.7	28	30	26
2.44 × 6.10	⊥[2] to ribs	1.22	1.22	30.6	34	39.8	36	39.3	34
Effect of diaphragm size									
2.44 × 6.10	⊥ to ribs	1.22	1.22	30.6	34	39.8	36	39.3	34
2.44 × 4.88	⊥ to ribs	1.22	1.22	37.0	23	44.4	22	45.4	22
Effect of spacing of end-fasteners									
2.44 × 4.88	⊥ to ribs	1.22	1.22	37.0	23	(end-fasteners spaced every 2nd valley)			
2.44 × 4.88	⊥ to ribs	1.22	1.22	31.5	32	(end-fasteners spaced every 3rd valley)			
Effect of 1.22 m × 1.05 m opening at midspan									
2.44 × 6.10	⊥ to ribs	1.22	1.22	30.6	34	39.8	36	39.3	34
2.44 × 6.10	⊥ to ribs	1.22	1.22	30.1	33	35.2[4]	29[4]	39.3	35

[1] Ribs fastened parallel to supporting truss chords or loading direction.
[2] Ribs fastened perpendicular to supporting truss chords or loading direction.
[3] Average of two tests of approximately the same values.
[4] Premature failure by withdrawal of nails at the compression edge beam.

Effect of length of diaphragm on strength and mode of failure

Three 2.44 m × 4.88 m (8 ft × 16 ft) diaphragms, with ribs perpendicular to the chords, were built and tested to investigate the effect of diaphragm length on strength and mode of failure. The results at failure were: aluminum, $P_u = 37$ kN (8,318 lb), $\Delta = 23$ mm (0.91 in.); steel 11 mm (7/16 in.) deep rib, $P_u = 44.4$ kN (9,982 lb), $\Delta = 22$ mm (0.87 in.); and steel 19 mm (3/4 in.) deep rib, $P_u = 45.4$ kN (10,207 lb), $\Delta = 22$ mm (0.087 in.). All three diaphragms failed at approximately the same deflection. The diaphragm built of aluminum was weaker by 20% than those of steel. The P_u–Δ relationships of these tests are shown in Fig. 8.

The mode of failure of the 4.88 m (16 ft) long diaphragms was similar to the mode of failure of the 6.10 m (20 ft) long diaphragms. Final failure of the steel diaphragms included local kinking along several ripples on end panels, and popping out of stitch screws. Final failure of the aluminum diaphragms included warping of the edge beams, local kinking along several ripples, and tearing around screw fasteners on end panels.

Effect of spacing of end-fasteners on strength and mode of failure

A 2.44 m × 4.88 m (8 ft × 16 ft) diaphragm built of aluminum with end-fasteners spaced every third valley instead of every second valley, used previously, was tested to observe the effect of spacing of end-fasteners on diaphragm strength and mode of failure. With end-fasteners spaced every third valley, P_u decreased by 15%, and Δ increased by 40% (Fig. 8). When the end-fasteners were spaced

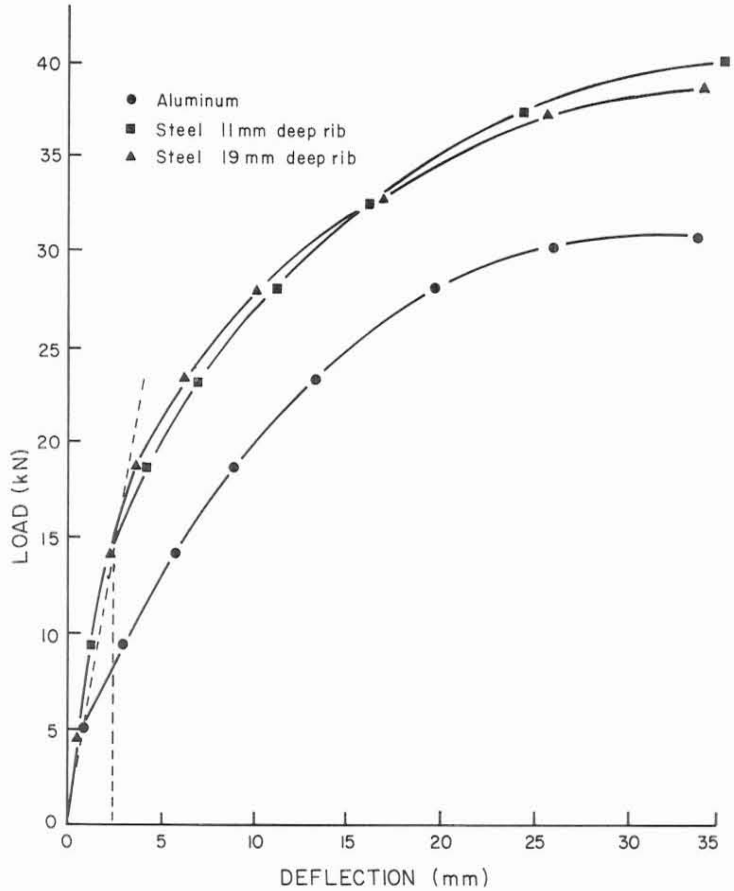

FIG. 7. Load-deflection relationships for 2.44 m × 6.10 m (8 ft × 20 ft) diaphragms when the ribs were perpendicular to the chords. Dotted lines show shear stiffness (P_u–Δ slope).

every third valley, failure occurred by buckling of the corrugation between fasteners at both ends of the diaphragm. When the end-fasteners were spaced every second valley, failure occurred by local buckling, tearing around end screws, and popping out. The number of ripples that started at the ends and propagated towards the center was doubled when the end-fasteners were spaced every third valley. The accordion-like warping can, therefore, be minimized by reducing the spacing of the end-fasteners. Since the extension of the warped region into the diaphragm appears to be a function of the spacing of the end-fasteners, there would be a relatively larger unwarped and rigid shear resisting area in the diaphragm as the length of the diaphragm is increased.

Effect of an opening on strength and mode of failure of diaphragms

In all of the tests discussed previously, the ripples started at the ends and gradually propagated but never reached the middle 1.22 m (4 ft) span. Thus, the logical place to make an opening in a ceiling diaphragm is at midspan or near midspan in order to retain the strength of the ceiling.

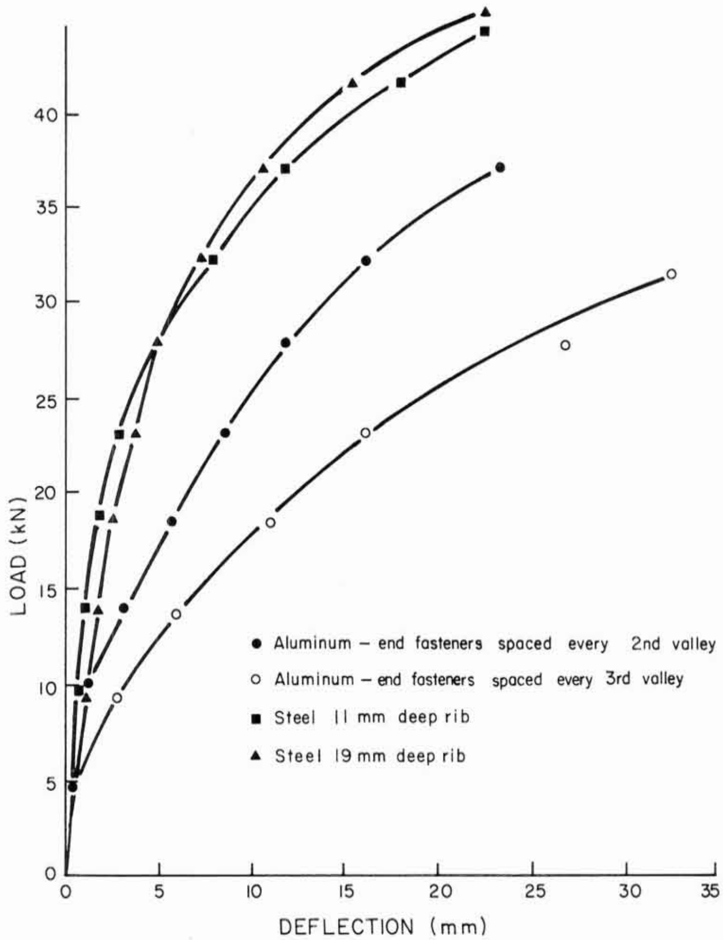

FIG. 8. Load-deflection relationships for 2.44 m × 4.88 m (8 ft × 16 ft) diaphragms when the ribs were perpendicular to the chords.

Three 2.44 m × 6.10 m (8 ft × 20 ft) diaphragms, one of each profile, were built with 1.22 m (4 ft) long by 1.05 m (3.5 ft) deep openings located at midspan. The panels were fastened perpendicular to the chords. The P_u–Δ relationships of these tests are shown in Fig. 9. The opening at midspan had no significant local or final effect on the ultimate load or mode of failure of the diaphragms tested. The load and midspan deflection at failure were: aluminum, $P_u = 30.1$ kN (6,767 lb), $\Delta = 33$ mm (1.30 in.); steel 11 mm (7/16 in.) deep rib, $P_u = 35.2$ kN* (7,914 lb), $\Delta = 29$ mm* (1.14 in.); and steel 19 mm (3/4 in.) deep rib, $P_u = 39.3$ kN (8,835 lb), $\Delta = 35$ mm (1.38 in.).

Practical implications of the data

The practical implication of the applied failure loads is that they can be related to wind loads that produce ceiling or roof diaphragm action. Using equations of

---

* Premature failure due to withdrawal of nails at the compression edge beam.

statics, the diaphragm ceiling may be critical for moment M_{max} near mid-length, or total shear force V_{max} near the ends, as follows:

$$M_{max} = \frac{wL^2}{8} = \left(q\frac{h}{2}\right)\frac{L^2}{8} \quad (1)$$

$$V_{max} = \frac{wL}{2} = \left(q\frac{h}{2}\right)\frac{L}{2} \quad (2)$$

where, q = design wind pressure, kN/m^2 (psf); h = wall height, m (ft), and L = ceiling length, m (ft). Eqs. (1) and (2) assume that roof horizontal force components cancel each other. Both equations are used to satisfy the design requirements of a diaphragm ceiling for horizontal wind bracing. In Eq. (2), if one assumes that the shear is uniform across the ceiling span W (m), and S (kN/m of span) is the shear strength of the ceiling, then

$$V = WS = 0.25qhL,$$

and

$$S = 0.25qh\frac{L}{W} \quad (3)$$

Thus, the required shear strength S for the ceiling assembly is a function of the design wind pressure q, wall height h, and the ceiling length-to-width ratio, L/W. Knowing the shear strength S, the number and spacing of end-fasteners required to safely carry the shear load can be calculated.

The lowest failure load found was 25.9 kN (5,823 lb). With shear governing, this is equivalent to 4.3 kN/m (291 lb/ft) or a wind pressure of 2.35 kN/m^2 (48.5 psf) on an assumed 3.66 m (12 ft) wall height. The highest failure load (45.4 kN or 10,207 lb) is equivalent to 7.44 kN/m (510 lb/ft) or a wind pressure of 4.1 kN/m^2 (85 psf) for 3.66 m (12 ft) wall height. The calculated wind pressure is based on the applied failure load, and thus does not include factor of safety.

SUMMARY

Ultimate Strength: Sixteen ceiling diaphragms of various assumptions were tested as deep beams under simulated wind loads. The loads at failure and midspan deflections of all the tests are given in Table 1. The applied failure loads exceeded by more than 2.5 times the design wind loads normally used in typical agricultural buildings. The load-deflection response was non-linear.

Material Strength: Diaphragms built of aluminum were weaker by 11 to 16% than those of steel when ribs were parallel to supporting chords, and by 29% when perpendicular. Both steel profiles exhibited identical strength and mode of failure.

Direction of Ribs: When ribs were parallel to the supporting chords, aluminum diaphragms were weaker by 18%, steel 11 mm (7/16 in.) deep rib by 24%, and steel 19 mm (3/4 in.) deep rib by 39% than their counterparts, when perpendicular.

Grid Size: Reducing the size of the supporting grid from 1.22 m × 1.22 m (4 ft × 4 ft) to 0.81 m × 1.22 m (2 ft 8 in. × 4 ft) resulted in a 25% increase in the ultimate load of the aluminum diaphragms. Reducing the grid size further to 0.61 m × 0.81 m (2 ft × 2 ft 8 in.) had no additional change.

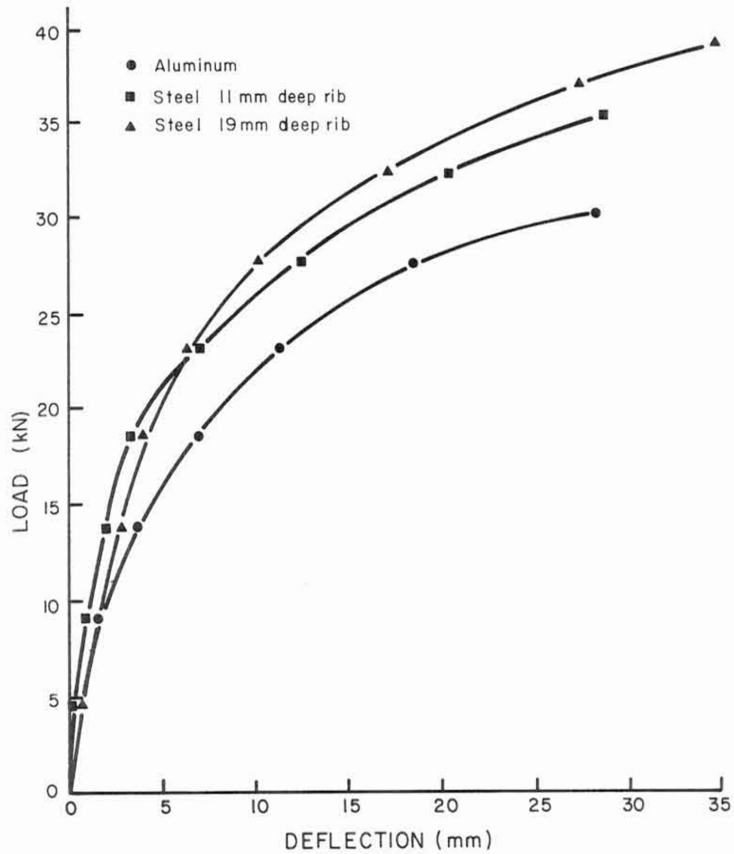

FIG. 9. Load-deflection relationships for 2.44 m × 6.10 m (8 ft × 20 ft) diaphragms with 1.22 m long × 1.05 m deep (4 ft × 3.5 ft) openings located at midspan.

Mode of Failure: The mode of failure was similar in all of the tests. Five to six ripples started at the ends of the diaphragms and propagated but never reached the middle 1.22 m (4 ft) span. Final failure was by local panel kinking along several ripples, and popping out of stitch screws and/or end-fasteners.

End-Fasteners: In the aluminum diaphragms, changing the spacing of the end-fasteners from every second valley to every third decreased the ultimate load by 15%, and increased midspan deflection by 40%.

Diaphragm Size: Increasing the diaphragm size from 2.44 m × 4.88 m (8 ft × 16 ft) to 2.44 m × 6.10 m (8 ft × 20 ft), decreased the ultimate load by 17%, and increased midspan deflection by 48% in aluminum, and decreased the load 10 to 13%, and increased deflection 55 to 64% in the steel. The mode of failure was the same in all cases.

An Opening at Midspan: A 1.22 m (4 ft) long by 1.05 m (3.5 ft) deep opening located at midspan of the 2.44 m × 6.10 m (8 ft × 20 ft) ceiling diaphragm had no significant effect on the strength, stability or mode of failure of the diaphragms tested.

ACKNOWLEDGMENTS

FABRAL–Alcan Building Products, Division of Alcan Aluminum Corporation, Lancaster, Pennsylvania, provided all the panels and fasteners used in this investigation.

REFERENCES

Gebremedhin, K. G., and F. E. Woeste. 1985. Diaphragm design with knee brace slip for post-frame buildings. Trans. of the ASAE 29(2): 538–542.

Hausman, C. T., and M. L. Esmay. 1977. The diaphragm strength of pole buildings. Transactions of the ASAE 30(1):114–116.

Hoagland, R. C., and D. S. Bundy. 1983. Strength and stiffness of screw-fastened roof panels for pole buildings. Transactions of the ASAE 26(2):512–515.

Johnston, R. A., and J. O. Curtis. 1984. Experimental verification of stressed-skin design of pole-frame buildings. Transactions of the ASAE 27(1):159–164.

Luttrell, L. D. 1967. Strength and behavior of light-gauge steel shear diaphragms. Cornell Research Bulletin 67-1.

Turnbull, J. E., K. C. McMartin, and A. T. Quaile. 1982. Structural performance of plywood and steel ceiling diaphragms. Can. Agr. Eng. 24(2):135–140.

White, R. N. 1978. Diaphragm-action of aluminum-clad timber-framed buildings. ASAE Paper No. 78-4501, ASAE, St. Joseph, MI.